ACS Synthetic Biology

Letter

An improved whole-cell biosensor for the discovery of lignin-transforming enzymes in functional metagenomic screens

Joe C.H. Ho, Sandip V. Pawar, Steven J. Hallam, and Vikramaditya G. Yadav

ACS Synth. Biol., **Just Accepted Manuscript** • DOI: 10.1021/acssynbio.7b00412 • Publication Date (Web): 28 Nov 2017

ACS Publications

ACS Synthetic Biology is published by the American Chemical Society. 1155 Sixteenth Street N.W., Washington, DC 20036

An improved whole-cell biosensor for the discovery of lignin-transforming enzymes in functional metagenomic screens

Joe C. H. Ho[1], Sandip V. Pawar[2], Steven J. Hallam[1*] & Vikramaditya G. Yadav[2*]

[1]Department of Microbiology and Immunology, University of British Columbia, Vancouver, BC, Canada

[2]Department of Chemical & Biological Engineering, University of British Columbia, Vancouver, BC, Canada

*Corresponding authors: Steven J. Hallam (shallam@mail.ubc.ca) and Vikramaditya G. Yadav (vikramaditya.yadav@ubc.ca)

Abstract

The discovery and utilization of biocatalysts that selectively valorize lignocellulose is critical to the profitability of next-generation biorefineries. Here, we report the development of a refactored, whole-cell, GFP-based biosensor for high-throughput identification of biocatalysts that transform lignin into speciality chemicals from environmental DNA of uncultivable archaea and bacteria. The biosensor comprises the transcriptional regulator and promoter of the emrRAB operon of *E. coli*, and the configuration of the biosensor was tuned with the aid of mathematical model. The biosensor sensitively and selectively detects vanillin and syringaldehyde, and responds linearly over a wide detection range. We employed the biosensor to screen 42,520 fosmid clones comprising environmental DNA isolated from two coal beds and successfully identified 147 clones that transform hardwood kraft lignin to vanillin and syringaldehyde.

Keywords

Lignin degradation, biosensors, functional metagenomic screening

There are an estimated 10^{30} prokaryotic microorganisms on the planet and the vast majority of this invisible majority remains uncultivated[1]. This represents both a challenge and an opportunity for the cultivation-independent discovery of biocatalysts that, if adequately harnessed, have enormous potential to drive the next generation of bio-based manufacturing[1–4]. The discovery of biocatalysts in environmental DNA of uncultivated bacteria, particularly those that selectively valorize specific substrates, presently proceeds by extracting, purifying, fragmenting and ligating the DNA into specialized vectors such as fosmids[5]. The DNA fragments typically range between 30- to 50-kilo base pairs in length. The fosmids are linearized, packaged into phage particles, and subsequently transduced into a suitable host such as phage-resistant *Escherichia coli* to produce a library of fosmid-bearing clones. The clones are later recovered and cultured on selected substrates to evaluate their catalytic potential using a variety of detection schemes[6–8]. Clones exhibiting the desired phenotype are investigated further to unambiguously determine the identity of the biocatalyst or biocatalytic cluster. Among the numerous detection schemes that are currently employed, of the use of whole-cell biosensors comprising regulatory elements of one-component transcriptional regulators has emerged as a favored tool, especially for high-throughput metabolite detection[6]. Whole-cell biosensors can detect lignin transformation at microliter volumes, which facilitates high-throughput screening that cannot otherwise be achieved with macro-scale analytical methodologies such as Klason analysis or gel permeation chromatography. In the case of assessing breakdown of lignin, the use of whole-cell biosensors also obviates the need for time-consuming steps such as derivatization[9] or modification of the analytes, as well as the use of ^{14}C-radioactively

labeled lignin[10,11], lignolytic indicator dyes[12] or fluorescently modified lignin[13].

The biosensor is typically expressed on a plasmid and comprises a fluorescent or luminescent reporter. The gene encoding the reporter is transcribed under the control of the promoter of a transcriptional regulator that is either endogenous to the biosensor host or is heterologously transferred to the host from a different bacterium. In the absence of the product in the intracellular milieu of the screening host, the regulator binds to its cognate promoter and represses transcription of the reporter gene. Binding of the product to the regulator induces a conformational change in the protein that de-represses transcription of the reporter gene. As a consequence, the biosensor functions by transducing intracellular product concentrations to a fluorescent or luminescent signal[14–16]. We previously constructed a one-component biosensor for the identification of novel biocatalysts that valorize lignin to two commercially important monoaromatic compounds, vanillin and syringaldehyde[17]. Lignin is a highly recalcitrant by-product of the deconstruction of lignocellulosic biomass[18]; and the development of cost-effective platforms that directly convert lignin into value-added products such as vanillin and syringaldehyde promises to greatly improve profitability of upgrading lignocellulose into biofuels and bioproducts[19]. Current commercial biosynthesis of both monoaromatic products occurs through multi-step, anabolic pathways[20], which greatly diminishes the yield and productivity of the bioprocesses that employ this scheme. Rather, the catabolic breakdown of lignin can directly generate these monoaromatic compounds at higher yields and productivities. Moreover, the breakdown products can also serve as intermediates to other renewable biochemicals[9,21,22], which further improves the

valorization quotient. The original lignin biosensor was identified by screening a library of over 1,820 *E. coli* clones, each of which harbors a plasmid bearing a transcriptional fusion of the green fluorescent protein (GFP) with a unique promoter from the bacterium[23], in the presence of selected monoaromatic compounds. This resulted in the recovery *emrRAB* operon promoter. The operon encodes a multi-drug efflux pump EmrAB under the transcriptional control of the regulator EmrR[24–26].

We subsequently cloned the transcriptional fusion of GFP with the promoter of the *emrRAB* operon into a specialized plasmid pCC1 (**Fig. 1A**) and transformed the construct (hereinafter referred to as P_{emrR}-gfp) into a phage-resistant strain EPI300 *E. coli* strain. This whole-cell biosensor was co-cultured with fosmid clones expressing environmental DNA sourced from two coal beds on solvent-treated hardwood kraft lignin (HWKL). We observed that as many as 24 clones activated the biosensor. The fluorescence measurements of the 24 clones using the pCC1 biosensor ranged from 104 ± 25 to 149 ± 0 fluorescence units, and differential levels of lignin transformation vanillin and syringaldehyde were confirmed by GC/MS (**Fig. 2**). Bioinformatics analysis of the fosmid sequences identified a number of different oxidoreductases, hydrolases, hydrogen peroxide-forming biocatalysts, as well as enzymes that catabolize and efflux aromatic compounds. Each of these enzyme types is known to play a role in the breakdown of lignin[27–29]. Nevertheless, of the 24 clones cultured in lignin-amended media, only 11 consistently induced the biosensor to levels above the negative control, an empty pCC1 fosmid (**Supplementary information, Fig. S1A**). The dissonance between the ability of the biosensor to consistently identify clones that synthesize

vanillin and syringaldehyde necessitated refinement of the biosensor. Moreover, we also observed that the detection range of the biosensor was quite narrow and it did not respond linearly to increasing concentrations of vanillin or syringaldehyde. These drawbacks could significantly limit the utility of the biosensor with respect to functional metagenomic screening and metabolic engineering to refine clones that produce vanillin and syringaldehyde most prolifically.

In order to improve the performance of the P_{emrR}-gfp biosensor, we formulated a mathematical model to relate its fluorescent output to biochemical parameters such as the concentrations of EmrR and EmrAB within the biosensor host, the fluxes of vanillin and syringaldehyde into and out of the host, as well as the rates of formation of the two compounds by the fosmid clones (**supplementary discussion**). The relationship between fluorescent output (S) and total vanillin concentration in the system (V_o) is described in **Eq. 1**.

$$\frac{dS}{dV_o} = \left[\frac{1}{\left(\frac{\gamma}{K_1 \cdot V_i \cdot R} \right) - K_2 - 1} \right] \quad (1)$$

The total vanillin concentration in the system is the summation of the concentrations of intracellular (V_i) and extracellular vanillin, as well as the intracellular concentrations of the complexes formed by vanillin with EmrR (R) and EmrAB. γ is the velocity with which lignin is catabolized by the fosmid clones. The break down of lignin is assumed to exhibit Michaelis-Menten kinetics. This assumption is in line with previously reported

data about ligninases[30–33]. The reaction rate constants (**Fig. 1B and Fig. S2**) for the binding of vanillin to EmrR and the subsequent de-repression of the *emrRAB* promoter are lumped into a single constant, K_1. These reactions are also assumed to exhibit Michaelis-Menten kinetics. The constant K_2 is the ratio of the reaction rate constant for the expression of the *emrRAB* operon and the rate constant for emission of the fluorescent signal. We also assumed the efflux of vanillin and syringaldehyde by EmrAB and the influx of the molecules into the biosensor host to be elementary rate processes. Likewise, the relationship between fluorescent output (S) and concentration of EmrR within the biosensor host is described in **Eq. 2**. β is the rate of constitutive expression of EmrR by the cell.

$$\frac{dS}{dR} = \left[\frac{1}{\left(\frac{\beta}{K_1 \cdot V_i \cdot R} \right) - 1} \right] \qquad (2)$$

Eqs. 1 and 2 clearly indicate that the sensitivity of the biosensor is closely tied to the intracellular concentration of EmrR – increasing the concentration of EmrR above constitutively expressed levels will improve sensitivity, but exceeding a threshold for the concentration will diminish the sensitivity. To test this hypothesis, we transformed the biosensor host with a pSB2K3 plasmid bearing an extra copy of the *emrR* gene that is transcribed under constitutive promoters from the Anderson promoter library (**Table S1**). We subsequently tested the biosensor by culturing the transformants in LB media at varying induction levels with vanillin (0 μM to 2.56 mM). Expectedly, the biosensor exhibited improved responsiveness and wider detection range. To determine the

optimality for the concentration of EmrR, we titrated the rate of transcription of *emrR* from the pSB2K3 plasmid by testing variants of constitutive promoters that transcribe the gene at varying strengths (**Fig. 1C**). We noticed a predictable improvement in the responsiveness and detection range as the strength of the transcriptional promoters increased (**Fig. 3**). However, as predicted by the mathematical model, we also observed that the performance of the biosensor was hampered when the strength of the promoters exceeded a threshold. Beyond increasing the intracellular concentration of EmrR, the mathematical model also points to increasing the copy number of *emr* promoters within the cell to improve sensitivity.

Based on these modeling results, we cloned the transcriptional fusion of GFP with the *emr* promoter into the pET15b plasmid and transformed into EPI300 cells with this construct to generate a new whole-cell biosensor. *E. coli* synthesizes and maintains as many as 500 copies of the pET15b plasmid. In comparison, only 50 copies of pCC1 are observed in the bacterium. The roughly 10-fold increase in the number of *emr* promoters within the host produced a significant increase in fluorescence output that distinctly and linearly correlated to inducer concentrations up to as high as 640 μM of total vanillin **(Fig. 4**). Importantly, unlike the pCC1 biosensor, the pET15b biosensor does not exhibit decay in fluorescence at higher concentrations of vanillin. Consistent with this observation, the pET15b biosensor performed better than the pCC1 biosensor when co-cultured in lignin-amended media with the 24 clones identified. As many as 19 clones induced the pET15b biosensor at statistically significant levels compared to the negative control (**Fig. S1B**). The enhancement in the fluorescent output was roughly

1.5-fold, ranging from 150 ± 9.8 to 249 ± 8.7 fluorescence units. This improvement in the pET15 biosensor provided a greater signal-to-noise ratio compared to the negative control, which resulted in an elevated distinction in fluorescence signals between fosmid clones. In addition, the pET15 biosensor also favors the growth of the biosensor host under a different antibiotic resistance marker in co-culture. As a consequence, the growth of the pET15 biosensor is normalized under ampicillin-induced media in fosmid library screening following the initial incubation of the fosmid clones with lignin.

To confirm the improved ability of the pET15b biosensor to identify biocatalysts that can selectively transform lignin, we deployed it to re-screen the 42,520 fosmid clones that were previously tested using the P_{emrR}-gfp biosensor. Under exactly the same assay conditions, pET15b biosensor detected 147 clones with the capacity to produce vanillin and syringaldehyde (**Fig. 5**). Intriguingly, each of the 147 new clones that were discovered in the experiment induced the biosensor at levels over 4 standard deviations higher than any of the previously identified 24 clones, suggesting that the re-designed sensor is substantially more responsive and sensitive, particularly at higher concentrations of vanillin and syringaldehyde. We confirmed this claim by evaluating 10 of these 147 clones for their ability to break down HWKL to vanillin and syringaldehyde more efficiently compared to clones identified using the previous generation of the biosensor. We selected 5 clones from each of the coal bed fosmid libraries and quantified the titers of vanillin and syringaldehyde using GC/MS (**Fig. 6**). All 10 clones that were evaluated exhibited increased vanillin and syringaldehyde production compared to the 24 clones that were identified by the first generation of the biosensor

and production was, on average, 3-fold higher. Finally, it has been previously reported that EmrR can also bind to other aromatic compounds[24–26]. These observations raise valid questions regarding the selectivity of the biosensor. Consequently, we evaluated the selectivity of the pET15b biosensor to vanillin and syringaldehyde by recording its response to increasing concentrations of 36 monoaromatic compounds that are putatively produced during the breakdown of lignin (**Fig. S3 and Table S2 in supplementary discussion**). We observed that the biosensor was activated by only vanillin and syringaldehyde, which not only confirms its high selectivity for functional groups (**Table S3**) within these specific classes of lignin-derived monoaromatic intermediates, but also validates the screening protocol that we implemented to identify EmrR through promoter-trap library screening.

In conclusion, by combining modeling and modular construction approaches, we successfully designed an improved one-component biosensor that is selectively responsive to lignin transformation products. Significantly, we have established a generalizable workflow for the design of whole-cell biosensors with increased responsiveness, sensitivity and linear detection range in *E. coli* that can be deployed effectively in functional metagenomic screens. Our results confirm the important role played by promoter strength[34,35], plasmid copy number[36] and regulator concentrations[37–39] in determining the performance of biosensors. The improved biosensor used in this study successfully identified 147 new clones that selectively degrade lignin into vanillin and syringaldehyde. Vanillin and syringaldehyde are important products in the breakdown of lignin and can be used as intermediates in the synthesis of other

important chemicals such as mucconic acid[9,21]. As we discover and later characterize more biocatalysts in our fosmid libraries, additional orthogonal biosensors[36] could be implemented in the search for intermediary biocatalysts that can consolidate the bioconversion of vanillin or syringaldehyde to the desired downstream products. Our work lays the foundations for deep device mining[6] of metagenomes for industrial biocatalysts, which will undoubtedly revolutionize bio-based chemical manufacturing.

Methods and materials

Whole-cell biosensor construction: The P_{emrR}-gfp promoter and GFP was amplified from the pCC1 P_{emrR}-gfp construct with the pET15_forward primer (caccggcgactagtCGCAGCATTATCATCC) and the pET15_reverse primer (agatctgctagcTATAAACGCAGAAAGGC). The PCR product was digested with SgrAI and BglII and then ligated to SgrAI/BglII-digested pET15 to generate the pET15 P_{emrR}-gfp biosensor. For fosmid co-culture and library screening, the pET15 P_{emrR}-gfp biosensor was co-transformed with an empty pCC1FOS in EPI300 *E.coli* cells to provide resistance to added chloramphenicol in the screen. The transcriptional regulator *emrR* was amplified from the *emrRAB* operon of *E.coli* K12 gDNA using the forward primer (gaattcgcggccgcttctagaTGGATAGTTCGTTTACGC) and reverse primer (ctgcagcggccgctactagtTTAGCTCATCGCTTCGAG). These biosensor constructs were transformed into E.cloni® 10G chemically competent cells. The PCR product amplified was digested with XbaI and PstI and then ligated behind a constitutive promoter sourced from the iGEM Biobrick registry (BBa_J23106, BBa_J23107, BBa_J23109,

BBa_J23113, BBa_J23114, or BBa_J23116) and a ribosomal binding site on SpeI/PstI-digested pSB2K3. pSB2K3-constitutively expressing *emrR* was co-transformed with pET15 P_{emrR}-gfp biosensor in E.cloni® 10G chemically competent cells to study the titrating effect of added expression of EmrR on the pET15 P_{emrR}-gfp biosensor .

Substrate screening and sensitivity measurements of the pET15 P_{emrR}-gfp biosensor: Substrate selectivity and sensitivity of the pET15 P_{emrR}-gfp biosensor were reported by measuring the GFP-fluorescence (481/520nm) normalized to cell density (OD_{600}) in the presence of chemical inducers. A single pET15 P_{emrR}-gfp colony was grown in LB media supplemented with ampicillin (100µg/mL) at 37°C for 18 hours. This biosensor culture was diluted (1:100) in 96-well black culture plates containing fresh LB media and chemical inducers supplemented at concentrations of 0µM, 20µM, 40µM, 80µM, 160µM, 320µM, 640µM, and 1.28mM. Measurements of fluorescence and cell density in the presence of each concentration of chemical inducer were performed in triplicates in 200uL. Microplates induced with chemicals were incubated at 30°C, with continuous orbital shaking, and monitored for GFP-fluorescence and cell density (OD_{600}) with a BioTek Synergy™ H1 multi-mode plate reader for 20 hours.

P_{emrR}-gfp biosensor performance in co-culture with fosmid clones in lignin-amended media : 0.5%(w/v) of lignin-amended LB media was prepared by adding 5 grams of hard-wood kraft lignin (HWKL) dissolved in DMSO (2% final concentration) to 1L of LB media. Lignin-amended LB media was stirred for 1 hour, and subsequently filtered by 0.2-µm filter (ExpressPlus; Milipore) to remove any remaining residues.

Selected single colonies of fosmid clones from coal-bed fosmid libraries were cultured in LB media supplemented with chloramphenicol (12.5µg/mL) and L-arabinose (100µg/mL) at 37°C for 18 hours. L-arabinose was added to induce the copy number of pCC1FOS. 100uL of the fosmid cultures were added to 96-well black coloured microplates in triplicates and subsequently induced with 50µL of lignin-amended LB media (0.5% w/v final concentration of HWKL) supplemented with chloramphenicol (12.5µg/mL) and L-arabinose (100µg/mL). Microplates induced with HWKL were incubated at 37°C for 24 hours, with continuous orbital shaking. 50uL of the pCC1 or pET15 P_{emrR}-gfp biosensor, diluted ¼ from an overnight culture in LB media was added to each well on the microplate. The pET15 P_{emrR}-gfp biosensor (cotransformed with an empty pCC1 vector) requires ampicillin (100µg/mL) selection; whereas the pCC1 P_{emrR}-gfp biosensor requires chloramphenicol (12.5µg/mL) selection. The microplate inoculated with wither pCC1 or pET15 P_{emrR}-gfp biosensor was then monitored for GFP-fluorescence (481/520nm) and cell density (OD_{600}) with a BioTek Synergy™ H1 multi-mode plate reader for 20 hours.

High-throughput fosmid library screening: Fosmid library screening was performed on the CO182 and CO183 coal-bed derived libraries, consisting of 46,000 clones organized in 384-well microplates. Fosmid clones were replicated using a Qpix2 robotic colony picker (Genetix) in 384-welll black microplates at an initial 30µL volume in LB media supplemented with chloramphenicol (12.5µg/mL) and L-arabinose (100µg/mL). When considering the volumes to be dispensed, a total of 5µL volume was considered to have evaporated every 24 hours. Microplates were incubated at 37°C for 24 hours to

provide initial growth to fosmid clones, and subsequently induced with 25µL of lignin-amended LB media (0.5% w/v final concentration of HWKL) supplemented with the same concentrations of chloramphenicol and L-arabinose. The microplates induced with HWKL were incubated at 37°C for an additional 48 hours prior to inoculation of the pET15 P_{emrR}-gfp biosensor. After 48 hours, an additional 40µL of LB supplemented with ampilicin (200µg/mL) was added to each well. The cotransformed pET15 P_{emrR}-gfp biosensor clone was inoculated to each microplate using the Qpix2 robotic colony picker. Initial GFP-fluorescence (481/520nm) and cell density (OD_{600}) was measured using the Thermo Scientific Varioskan^{TM} Flash multimode reader with the aid of microplate robotic stacker. Final GFP-fluorescence (481/520nm) and cell density (OD_{600}) were measured after 24 hours of incubation with the pET15 P_{emrR}-gfp biosensor at 37°C. Fosmid clones that significantly activated the biosensor were identified by ranking their robust Z-scores, a standard calculation used in high-throughput screening that is insensitive to strong outliers[40–42]. Robust Z-score measurements were calculated from the fold-increase in fluorescence of each well.

Acknowledgements

We would like to thank Rahul Singh, Lindsay Eltis and Steve Withers for insightful conversations regarding biomass deconstruction and the future of biorefining. We also thank Payal Sipahimalani, Melanie Scofield, and Sam Kheirandish for technical support related to library production. This work was performed under the auspices of the Natural Sciences and Engineering Research Council (NSERC) of Canada, Canada Foundation

for Innovation (CFI) and the Canadian Institute for Advanced Research (CIFAR). JH was supported by the NSERC CREATE training program, Ecosystem Services, Commercialization Platforms and Entrepreneurship (ECOSCOPE).

Author contributions

SH and VY designed the study; JH and SP conducted the experiments; JH, SP, SH and VY analyzed the data; and JH and VY wrote the manuscript.

Online supplementary information

A description of the chemicals and reagents used in the study, analysis and validation of the desired lignolytic activity of the clones using GC-MS, development of the mathematical model for guided improvement of the biosensor and a listing of the promoter sequences is listed in the online supplementary information package.

References

(1) Whitman, W. B., Coleman, D. C., and Wiebe, W. J. (1998) Prokaryotes: the unseen majority. *Proc Natl Acad Sci U S A 95*, 6578–6583.

(2) Keller, M., and Zengler, K. (2004) Tapping into microbial diversity. *Nat. Rev. Microbiol. 2*, 141–150.

(3) Lorenz, P., and Eck, J. (2005) Metagenomics and industrial applications. *Nature 3*,

510–516.

(4) Yadav, V. G., and Stephanopoulos, G. (2014) Metabolic engineering: the ultimate paradigm for continuous pharmaceutical manufacturing. *ChemSusChem 7*, 1847–1853.

(5) Taupp, M., Lee, S., Hawley, A., Yang, J., and Hallam, S. (2009) Large insert environmental genomic library production. *J Vis Exp. 31*, 1387.

(6) Armstrong, Z., Mewis, K., Strachan, C., and Hallam, S. J. (2015) Biocatalysts for biomass deconstruction from environmental genomics. *Curr. Opin. Chem. Biol. 29*, 18–25.

(7) Mewis, K., Armstrong, Z., Song, Y. C., Baldwin, S. A., Withers, S. G., and Hallam, S. J. (2013) Biomining active cellulases from a mining bioremediation system. *J. Biotechnol. 167*, 462–471.

(8) Taupp, M., Mewis, K., and Hallam, S. J. (2011) The art and design of functional metagenomic screens. *Curr. Opin. Biotechnol. 22*, 465–472.

(9) Salvachúa, D., Karp, E. M., Nimlos, C. T., Vardon, D. R., and Beckham, G. T. (2015) Towards lignin consolidated bioprocessing: simultaneous lignin depolymerization and product generation by bacteria. *Green Chem. 17*, 4951–4967.

(10) Zimmermann, W. (1990) Degradation of lignin by bacteria. *J. Biotechnol.*

(11) Scheu, S. (1992) Decomposition of lignin in soil microcompartments: A methodical study with three different C-14-labelled lignin substrates. *Biol. Fertil. Soils 13*, 160–164.

(12) Bandounas, L., Wierckx, N. J., de Winde, J. H., and Ruijssenaars, H. J. (2011) Isolation and characterization of novel bacterial strains exhibiting ligninolytic potential. *BMC Biotechnol. 11*, 94.

(13) Ahmad, M., Taylor, C. R., Pink, D., Burton, K., Eastwood, D., Bending, G. D., and

Bugg, T. D. H. (2010) Development of novel assays for lignin degradation: comparative analysis of bacterial and fungal lignin degraders. *Mol. Biosyst. 6*, 815–821.

(14) Fernandez-López, R., Ruiz, R., de la Cruz, F., and Moncalián, G. (2015) Transcription factor-based biosensors enlightened by the analyte. *Front. Microbiol. 6*, 648.

(15) Ulrich, L. E., Koonin, E. V, and Zhulin, I. B. (2005) One-component systems dominate signal transduction in prokaryotes. *Trends Microbiol 13*, 52–56.

(16) Marijuán, P. C., Navarro, J., and del Moral, R. (2010) On prokaryotic intelligence: Strategies for sensing the environment. *BioSystems 99*, 94–103.

(17) Strachan, C. R., Singh, R., VanInsberghe, D., Ievdokymenko, K., Budwill, K., Mohn, W. W., Eltis, L. D., and Hallam, S. J. (2014) Metagenomic scaffolds enable combinatorial lignin transformation. *Proc Natl Acad Sci U S A 111*, 10143–10148.

(18) Himmel, M. E., Ding, S.-Y., Johnson, D. K., Adney, W. S., Nimlos, M. R., Brady, J. W., and Foust, T. D. (2007) Biomass recalcitrance: Engineering plants and enzymes for biofuels production. *Science 315*, 804–807.

(19) Ruiz-Dueñas, F., and Martínez, A. (2009) Microbial degradation of lignin: How a bulky recalcitrant polymer is efficiently recycled in nature and how we can take advantage of this. *Microb Biotechnol 2*, 164–177.

(20) Gallage, N., and Møller, B. (2015) Vanillin: Bioconversion and bioengineering of the most popular plant flavor and its de novo biosynthesis in the vanilla orchid. *Mol. Plant 8*, 40–57.

(21) Vardon, D. R., Franden, A., Johnson, C. W., Karp, E. M., Guarnieri, M. T., Linger, J. G., Salm, M. J., Strathmann, J., and Beckham, G. T. (2015) Adipic acid production from

lignin. *Energy Environ. Sci.* 617–628.

(22) Linger, J. G., Vardon, D. R., Guarnieri, M. T., Karp, E. M., Hunsinger, G. B., Franden, M. A., Johnson, C. W., Chupka, G., Strathmann, T. J., Pienkos, P. T., and Beckham, G. T. (2014) Lignin valorization through integrated biological funneling and chemical catalysis. *Proc. Natl. Acad. Sci.*

(23) Zaslaver, A., Bren, A., Ronen, M., Itzkovitz, S., Kikoin, I., Shavit, S., Liebermeister, W., Surette, M. G., and Alon, U. (2006) A comprehensive library of fluorescent transcriptional reporters for Escherichia coli. *Nat. Methods 3*, 623–628.

(24) Lomovskaya, O., Lewis, K., and Matin, a. (1995) EmrR is a negative regulator of the Escherichia coli multidrug resistance pump emrAB. *J. Bacteriol. 177*, 2328–2334.

(25) Xiong, a., Gottman, a., Park, C., Baetens, M., Pandza, S., and Matin, a. (2000) The EmrR protein represses the Escherichia coli emrRAB multidrug resistance operon by directly binding to its promoter region. *Antimicrob. Agents Chemother. 44*, 2905–2907.

(26) Brooun, a, Tomashek, J. J., and Lewis, K. (1999) Purification and ligand binding of EmrR, a regulator of a multidrug transporter. *J. Bacteriol. 181*, 5131–5133.

(27) Bugg, T., Ahmad, M., Hardiman, E., and Rahmanpour, R. (2011) Pathways for degradation of lignin in bacteria and fungi. *Nat Prod Rep 28*, 1883–1896.

(28) Brown, M., Barros, T., and Chang, M. (2012) Identification and characterization of a multifunctional dye peroxidase from a lignin-reactive bacterium. *ACS Chem Biol 7*, 2074–2081.

(29) Brown, M., and Chang, M. (2014) Exploring bacterial lignin degradation. Curr Opin Chem Biol 19:1–7. *Curr Opin Chem Biol 19*, 1–7.

(30) Harwardt, N., Stripling, N., Roth, S., Liu, H., Schwaneberg, U., and Spiess, A. C. (2014) Effects of ionic liquids on the reaction kinetics of a laccase–mediator system. *RSC Adv.*

(31) Fernández-Fueyo, E., Ruiz-Dueñas, F. J., and Martínez, A. T. (2014) Engineering a fungal peroxidase that degrades lignin at very acidic pH. *Biotechnol. Biofuels*.

(32) Chen, C., Shrestha, R., Jia, K., Gao, P. F., Geisbrecht, B. V., Bossmann, S. H., Shi, J., and Li, P. (2015) Characterization of dye-decolorizing peroxidase (DyP) from Thermomonospora curvata reveals unique catalytic properties of A-type DyPs. *J. Biol. Chem.*

(33) Ahmad, M., Roberts, J. N., Hardiman, E. M., Singh, R., Eltis, L. D., and Bugg, T. D. H. (2011) Identification of DypB from rhodococcus jostii RHA1 as a lignin peroxidase. *Biochemistry*.

(34) McNerney, M. P., Watstein, D. M., and Styczynski, M. P. (2015) Precision metabolic engineering: The design of responsive, selective, and controllable metabolic systems. *Metab. Eng.*

(35) Jha, R. K., Kern, T. L., Fox, D. T., and Strauss, C. E. M. (2014) Engineering an Acinetobacter regulon for biosensing and high-throughput enzyme screening in E. coli via flow cytometry. *Nucleic Acids Res.*

(36) Rogers, J. K., Guzman, C. D., Taylor, N. D., Raman, S., Anderson, K., and Church, G. M. (2015) Synthetic biosensors for precise gene control and real-time monitoring of metabolites. *Nucleic Acids Res.* gkv616.

(37) Xue, H., Shi, H., Yu, Z., He, S., Liu, S., Hou, Y., Pan, X., Wang, H., Zheng, P., Cui, C., Viets, H., Liang, J., Zhang, Y., Chen, S., Zhang, H. M., and Ouyang, Q. (2014)

Design, construction, and characterization of a set of biosensors for aromatic compounds. *ACS Synth. Biol.*

(38) Wang, B., Barahona, M., and Buck, M. (2015) Amplification of small molecule-inducible gene expression via tuning of intracellular receptor densities. *Nucleic Acids Res.*

(39) Merulla, D., Hatzimanikatis, V., and Van der Meer, J. R. (2013) Tunable reporter signal production in feedback-uncoupled arsenic bioreporters. *Microb. Biotechnol.*

(40) Goktug, A. N., Chai, S. C., and Chen, T. (2013) Data Analysis Approaches in High Throughput Screening, in *Drug Discovery*.

(41) Malo, N., Hanley, J., and Cerquozzi, S. (2006) Statistical practice in high-throughput screening data analysis. *Nat. Biotechnol.*

(42) Birmingham, A., Selfors, L. M., Forster, T., Wrobel, D., Kennedy, C. J., Shanks, E., Santoyo-Lopez, J., Dunican, D. J., Long, A., Kelleher, D., Smith, Q., Beijersbergen, R. L., Ghazal, P., and Shamu, C. E. (2009) Statistical methods for analysis of high-throughput RNA interference screens. *Nat Methods*.

Figure legends

Fig. 1. P_{emrR}-gfp biosensor design and operation. **A.** The promoter-operator sequence of the *emrRAB* operon was inserted upstream of GFP on a pCC1 fosmid. The transcriptional regulator EmrR is expressed endogenously by *E. coli*, and binds to the promoter-operator sequence of *emrRAB.* The binding of EmrR to the promoter-operator sequence of the P_{emrR}-gfp biosensor represses transcription of GFP ('OFF state'). Upon induction by monoaromatic compounds such as vanillin, the EmrR transcriptional regulator is de-repressed, which initiates GFP ('ON state'). **B.** The 'ON' and 'OFF' states of the biosensor, represented by the enzyme kinetics of each part of the system. Binding of intracellular vanillin (V_i) to the regulator is a prerequisite for signal activation. **C.** The P_{emrR}-gfp whole-cell biosensor was co-transformed with the plasmid pSB2K3. The latter expresses EmrR under the control of constitutive promoters from the Anderson promoter library.

Fig. 2. GC-MS confirmation of vanillin and syringaldehyde production. The fosmid clones were cultured on 0.5% (w/v) HWKL for 48 hours.

Fig. 3. Altering the dynamic range of the P_{emrR}-gfp biosensor by titrating the expression of EmrR transcriptional regulator. The P_{emrR}-gfp biosensor host was co-transformed with the pSB2K3 plasmids that express EmrR at varying levels owing to differential transcriptional control by variants of constitutive promoters from the Anderson promoter library. Normalized GFP fluorescence (GFP/OD_{600}) was measured for increasing

concentrations of vanillin, ranging from 0 μM to 2.56 mM.

Fig. 4. P_{emrR}-gfp biosensor sensitivity under high copy plasmid (pET15) versus lower copy plasmid (pCC1). Normalized GFP fluorescence (GFP/OD_{600}) was measured under increasing concentrations of vanillin, ranging from 0 μM to 640 μM.

Fig. 5. Metagenomic screening of coal-bed fosmid libraries, CO182 and CO183. CO182 and CO183 fosmid libraries were replicated in 384 well microplates and grown with 0.5% (v/w) HWKL for 48 hours followed by co-culture with the pET15 P_{emrR}-gfp biosensor for 24 hours. Fluorescence measurements were recorded and normalized for plate-to-plate effects by robust Z-scores calculations.

Fig 6. GC-MS confirmation of vanillin and syringaldehyde production on selected fosmid clones recovered in the re-screen with the improved pET15 biosensor. The top-5 fosmid clones (with the highest robust Z-score values) from each of the two coal bed libraries were chosen for GC-MS analysis. These fosmid clones were cultured on 0.5% (w/v) HWKL for 48 hours prior to extraction.

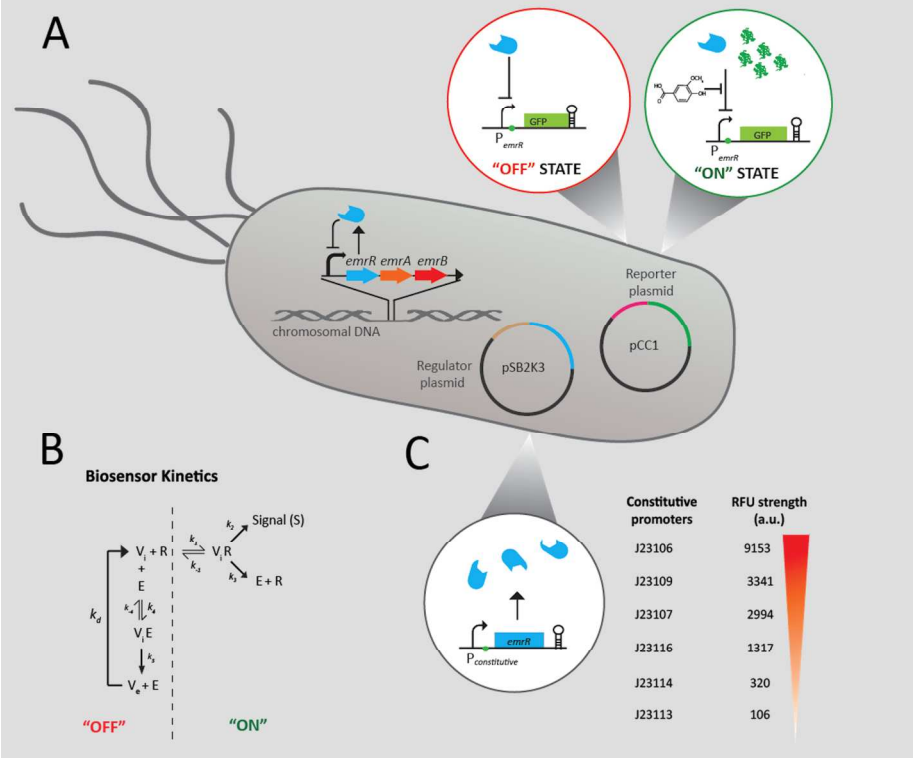

Fig. 1. P_{emrR}-gfp biosensor design and operation. **A.** The promoter-operator sequence of the *emrRAB* operon was inserted upstream of GFP on a pCC1 fosmid. The transcriptional regulator EmrR is expressed endogenously by *E. coli*, and binds to the promoter-operator sequence of *emrRAB.* The binding of EmrR to the promoter-operator sequence of the P_{emrR}-gfp biosensor represses transcription of GFP ('OFF state'). Upon induction by monoaromatic compounds such as vanillin, the EmrR transcriptional regulator is de-repressed, which initiates GFP ('ON state'). **B.** The 'ON' and 'OFF' states of the biosensor, represented by the enzyme kinetics of each part of the system. Binding of intracellular vanillin (V_i) to the regulator is a prerequisite for signal activation. **C.** The P_{emrR}-gfp whole-cell biosensor was co-transformed with the plasmid pSB2K3. The latter expresses EmrR under the control of constitutive promoters from the Anderson promoter library.

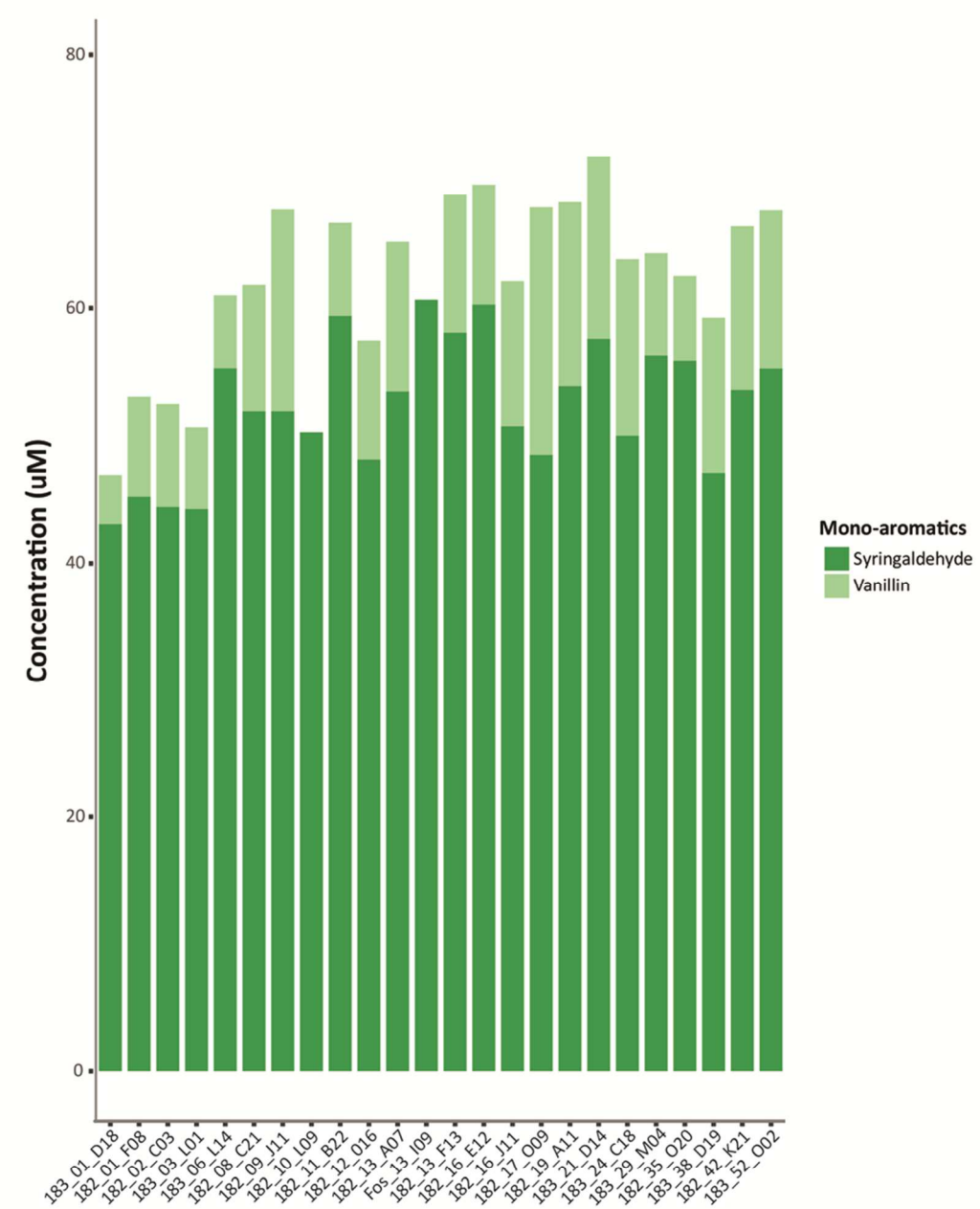

Fig. 2. GC-MS confirmation of vanillin and syringaldehyde production. The fosmid clones were cultured on 0.5% (w/v) HWKL for 48 hours.

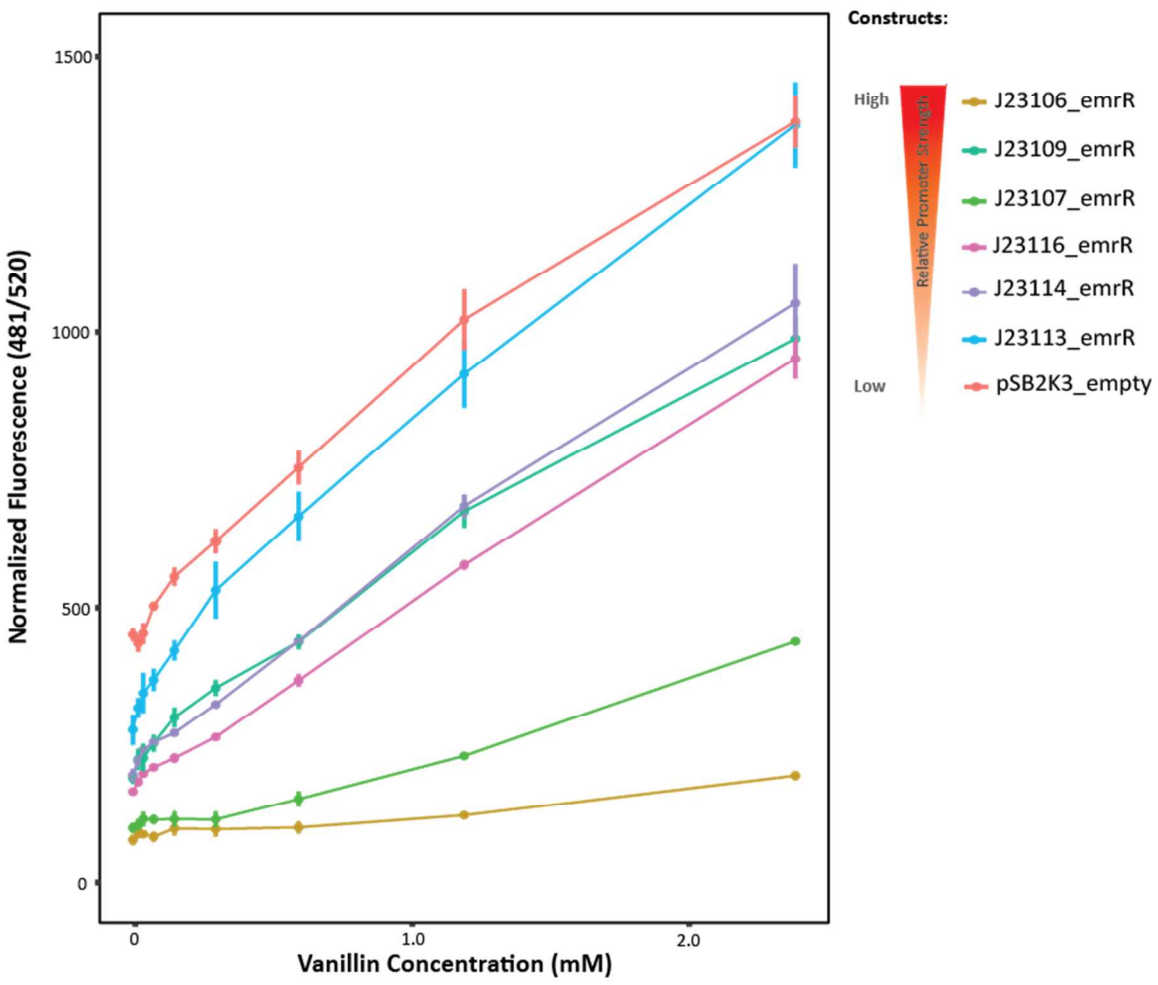

Fig. 3. Altering the dynamic range of the P_{emrR}-gfp biosensor by titrating the expression of EmrR transcriptional regulator. The P_{emrR}-gfp biosensor host was co-transformed with the pSB2K3 plasmids that express EmrR at varying levels owing to differential transcriptional control by variants of constitutive promoters from the Anderson promoter library. Normalized GFP fluorescence (GFP/OD_{600}) was measured for increasing concentrations of vanillin, ranging from 0 μM to 2.56 mM.

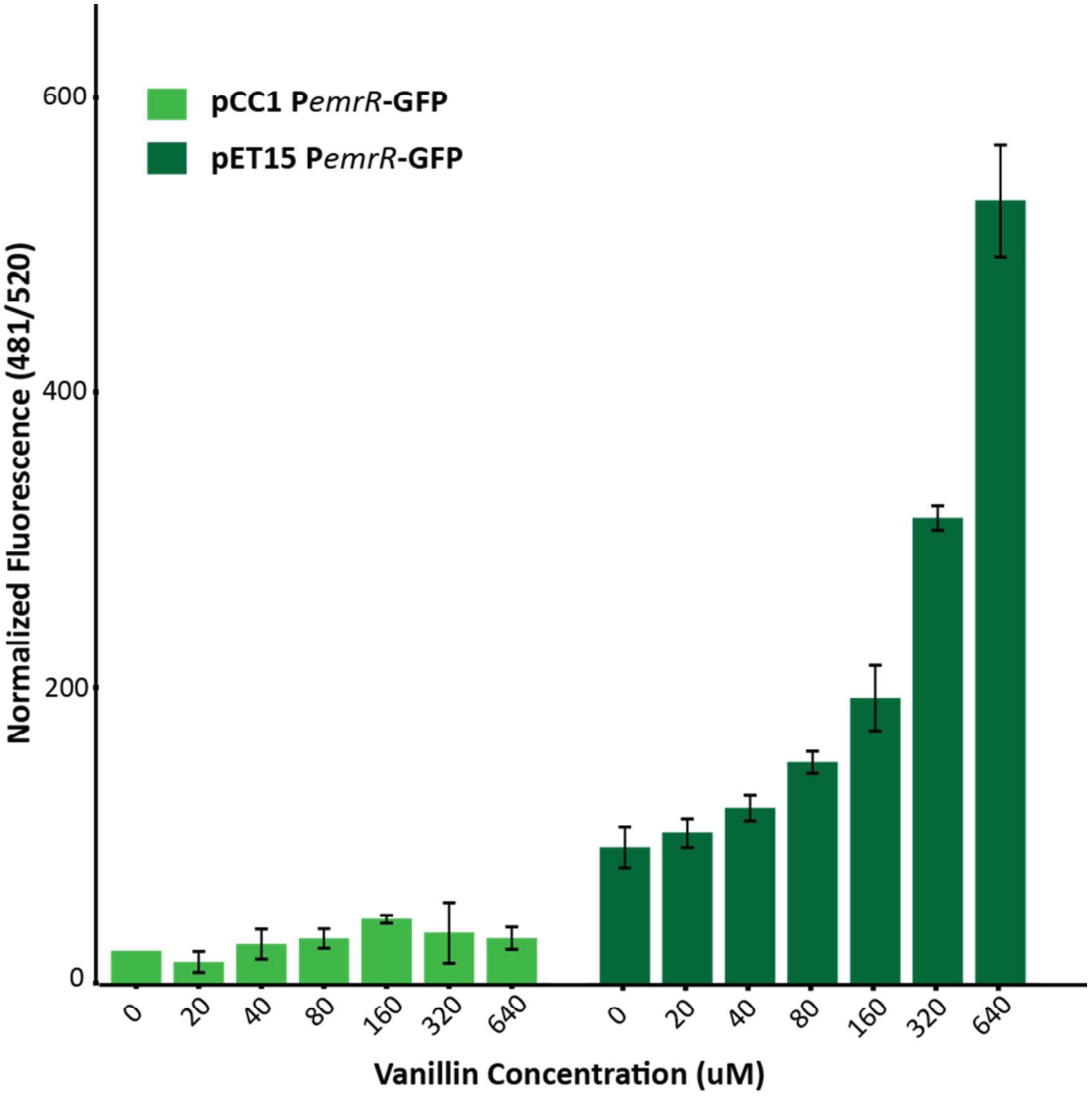

Fig. 4. P_{emrR}-gfp biosensor sensitivity under high copy plasmid (pET15) versus lower copy plasmid (pCC1). Normalized GFP fluorescence (GFP/OD_{600}) was measured under increasing concentrations of vanillin, ranging from 0 μM to 640 μM.

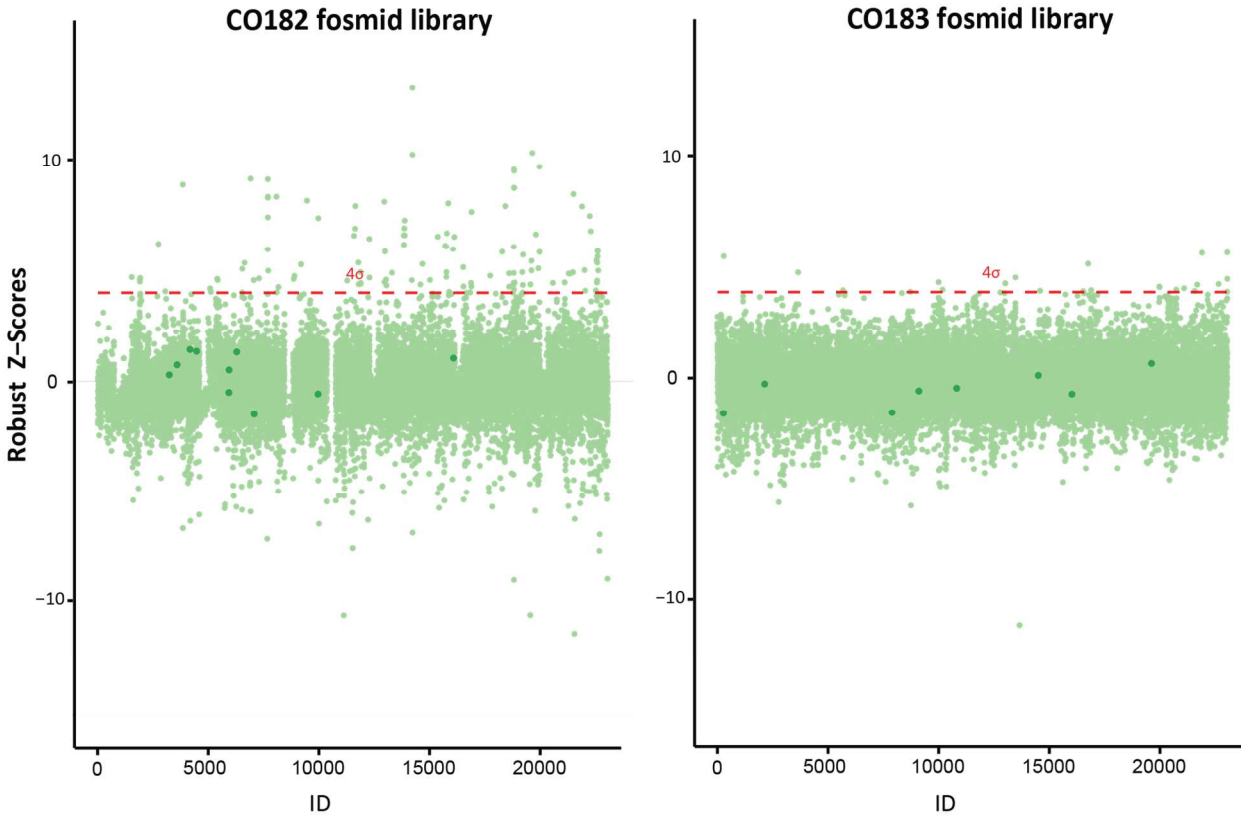

Fig. 5. Metagenomic screening of coal-bed fosmid libraries, CO182 and CO183. CO182 and CO183 fosmid libraries were replicated in 384 well microplates and grown with 0.5% (v/w) HWKL for 48 hours followed by co-culture with the pET15 P_{emrR}-gfp biosensor for 24 hours. Fluorescence measurements were recorded and normalized for plate-to-plate effects by robust Z-scores calculations.

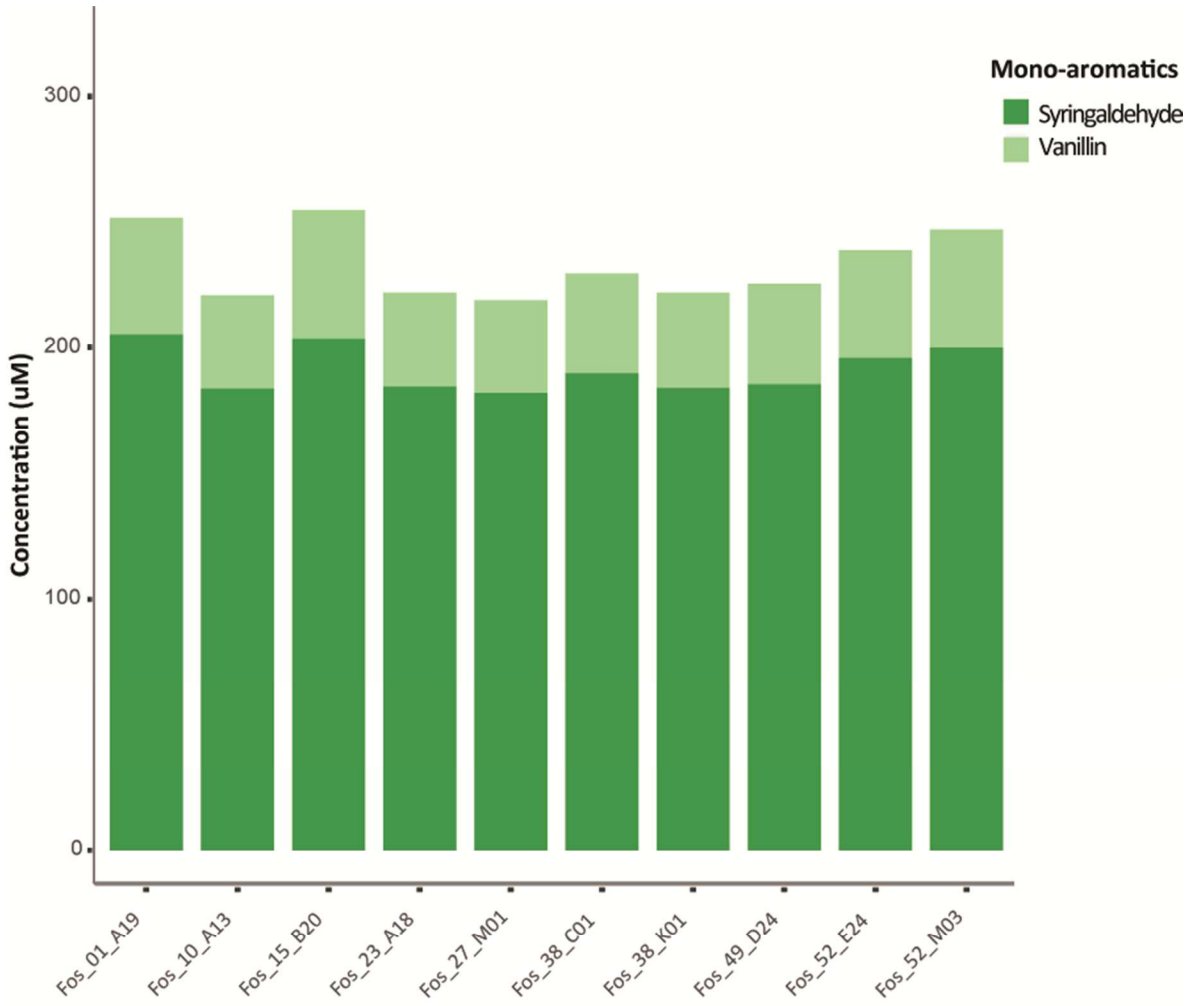

Fig 6. GC-MS confirmation of vanillin and syringaldehyde production on selected fosmid clones recovered in the re-screen with the improved pET15 biosensor. The top-5 fosmid clones (with the highest robust Z-score values) from each of the two coal bed libraries were chosen for GC-MS analysis. These fosmid clones were cultured on 0.5% (w/v) HWKL for 48 hours prior to extraction.

Table of contents image

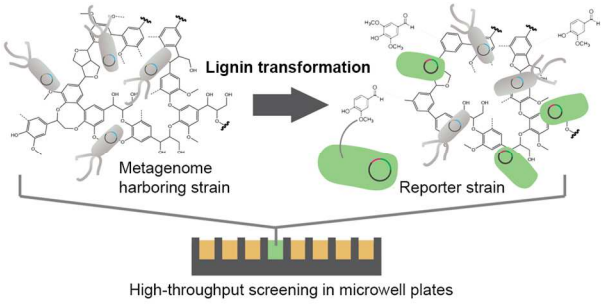

Online supplementary information contents

Fig. S1. Comparison between the pCC1 P_{emrR}-GFP and pET15 P_{emrR}-GFP biosensors. 24 fosmid-bearing *E. coli* clones were evaluated for their ability to activate pCC1 P_{emrR}-GFP biosensor (**A**) and pET15 P_{emrR}-GFP biosensor (**B**) following incubation with HWKL. The fluorescence readout is normalized to OD_{600} values.

Fig S2. Altering the dynamic range of the pET15 P_{emrR}-GFP biosensor by titrating the expression of EmrR transcriptional regulator. Expression of *emrR* was titrated by differential strengths of constitutive promoters and co-transformed with the pET15 P_{emrR}-GFP biosensor in *E.coli* cloni cells. Each co-expressed clone was tested at concentrations ranging from 0μM to 2.56mM vanillin and measured for its GFP fluorescence and cell density (OD_{600}). As the expression of EmrR increased, normalized GFP fluorescence (to cell density) decreased at the each concentration.

Fig. S3. We evaluated the selectivity of the pET15b biosensor by recording its response to increasing concentrations of 36 monoaromatic compounds that are putatively produced during the breakdown of lignin and determined that the biosensor was exclusively selective towards vanillin and syringaldehyde.

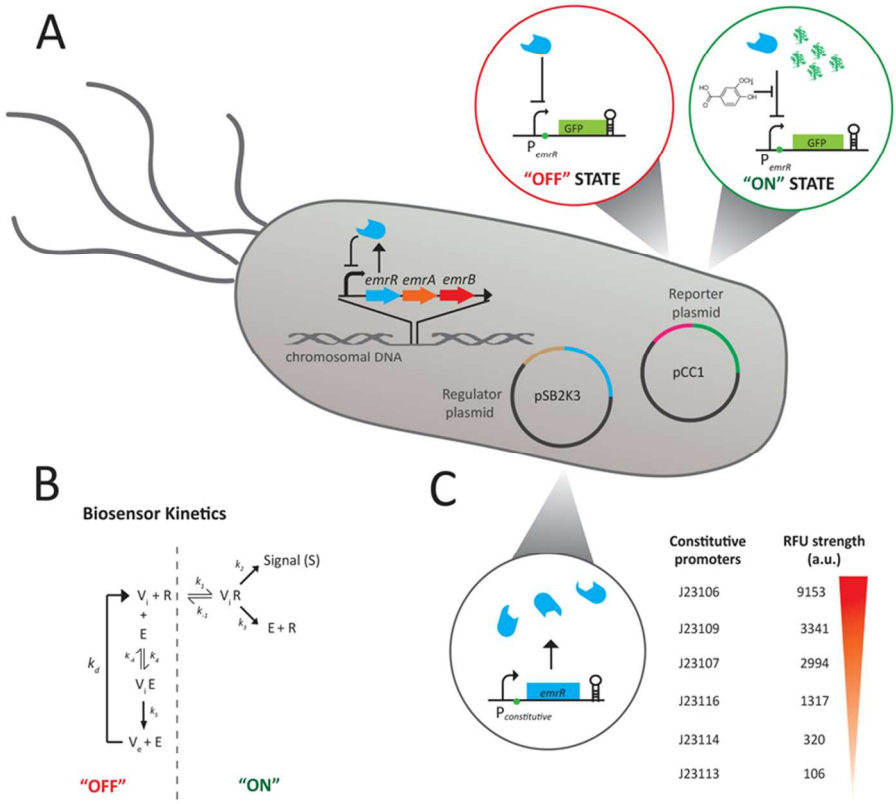

PemrR-GFP biosensor design and operation. A. The promoter-operator sequence of the emrRAB operon was inserted upstream of GFP on a pCC1 fosmid. The transcriptional regulator EmrR is expressed endogenously by E. coli, and binds to the promoter-operator sequence of emrRAB. The binding of EmrR to the promoter-operator sequence of the PemrR-GFP biosensor represses transcription of GFP ('OFF state'). Upon induction by monoaromatic compounds such as vanillin, the EmrR transcriptional regulator is de-repressed, which initiates GFP ('ON state'). B. The 'ON' and 'OFF' states of the biosensor, represented by the enzyme kinetics of each part of the system. Binding of intracellular vanillin (Vi) to the regulator is a prerequisite for signal activation. C. The PemrR-GFP whole-cell biosensor was co-transformed with the plasmid pSB2K3. The latter expresses EmrR under the control of constitutive promoters from the Anderson promoter library.

82x74mm (300 x 300 DPI)

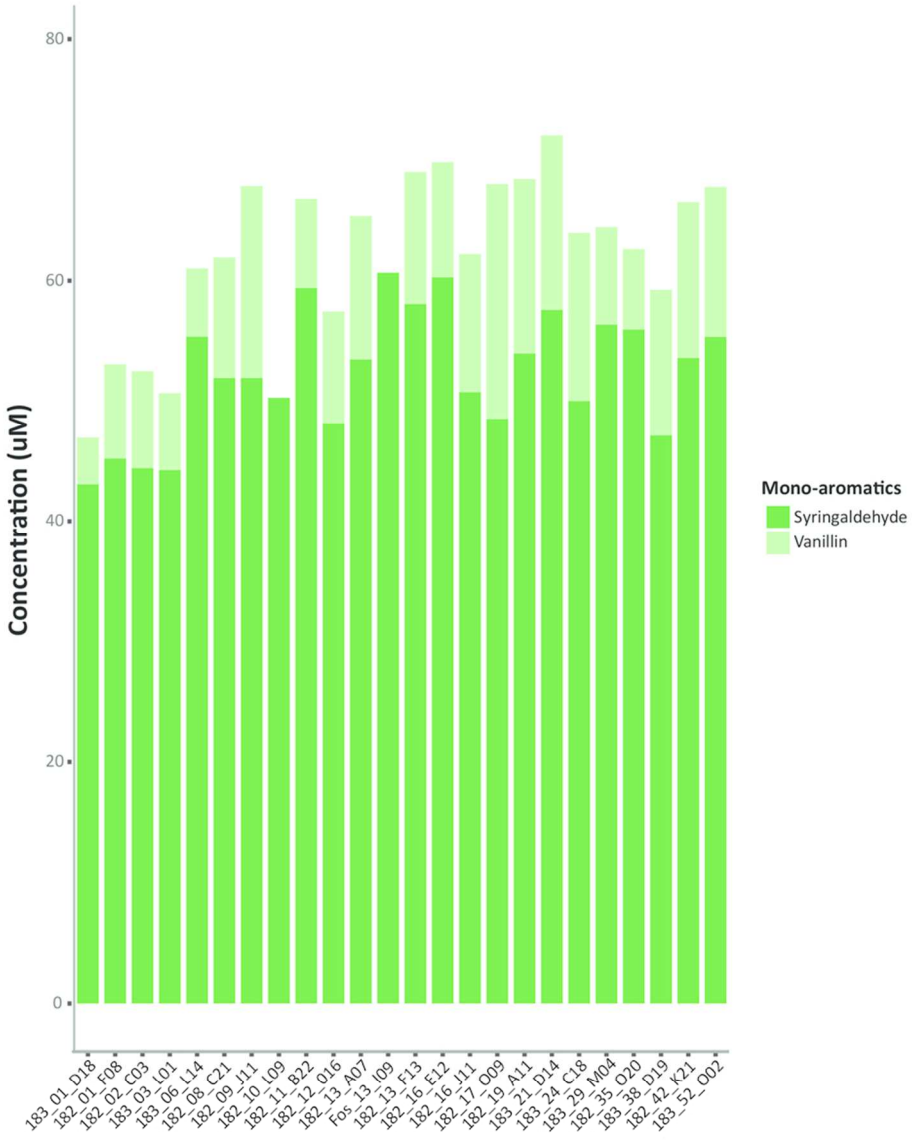

GC-MS confirmation of vanillin and syringaldehyde production. The fosmid clones were cultured on 0.5% (w/v) HWKL for 48 hours.

82x104mm (300 x 300 DPI)

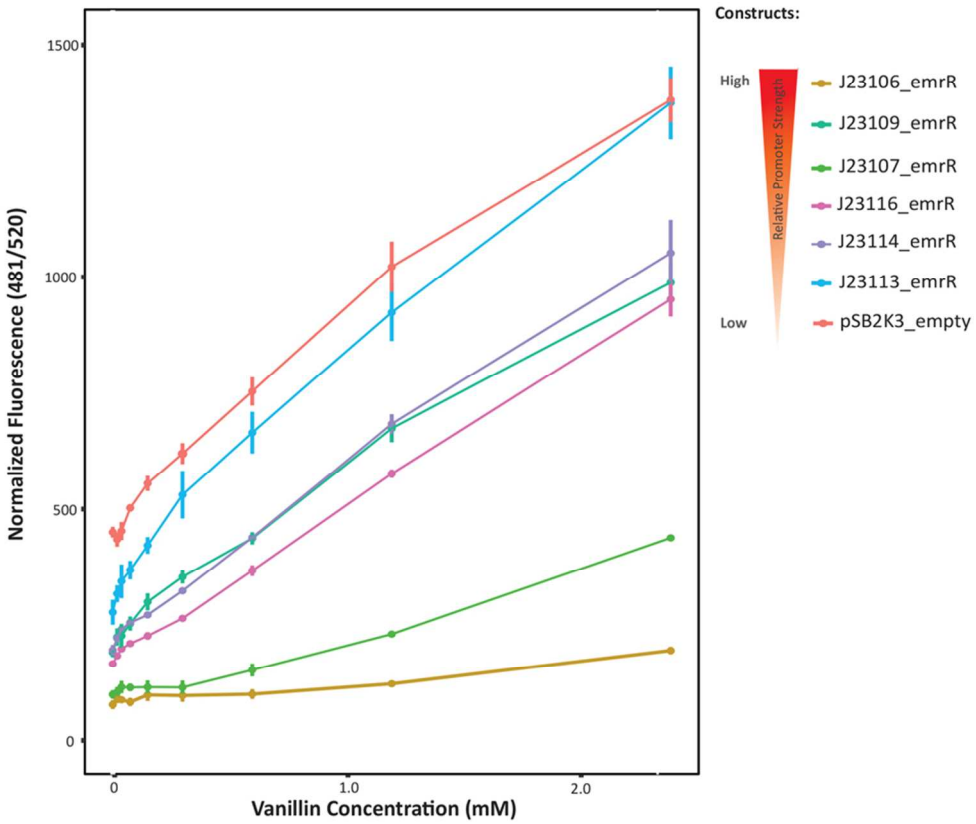

Altering the dynamic range of the PemrR-gfp biosensor by titrating the expression of EmrR transcriptional regulator. The PemrR-gfp biosensor host was co-transformed with the pSB2K3 plasmids that express EmrR at varying levels owing to differential transcriptional control by variants of constitutive promoters from the Anderson promoter library. Normalized GFP fluorescence (GFP/OD600) was measured for increasing concentrations of vanillin, ranging from 0 μM to 2.56 mM.

82x72mm (300 x 300 DPI)

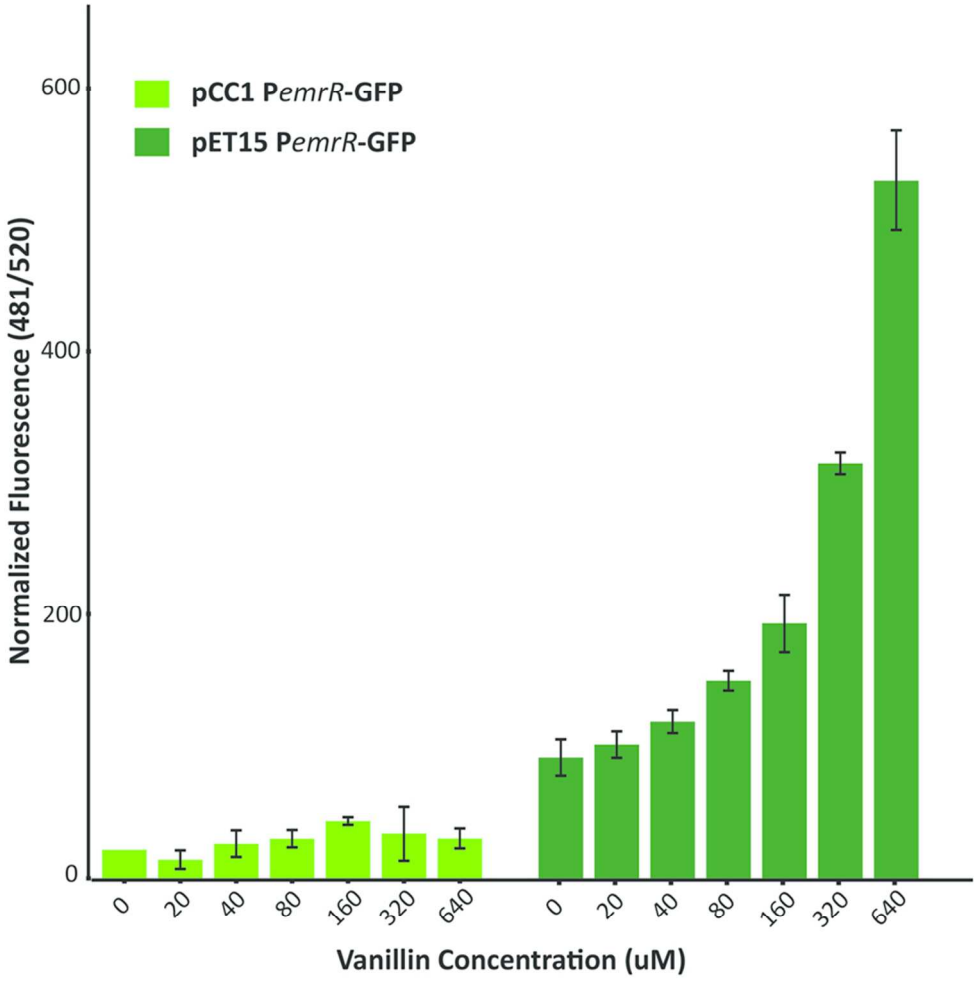

PemrR-gfp biosensor sensitivity under high copy plasmid (pET15) versus lower copy plasmid (pCC1). Normalized GFP fluorescence (GFP/OD600) was measured under increasing concentrations of vanillin, ranging from 0 μM to 640 μM.

82x85mm (300 x 300 DPI)

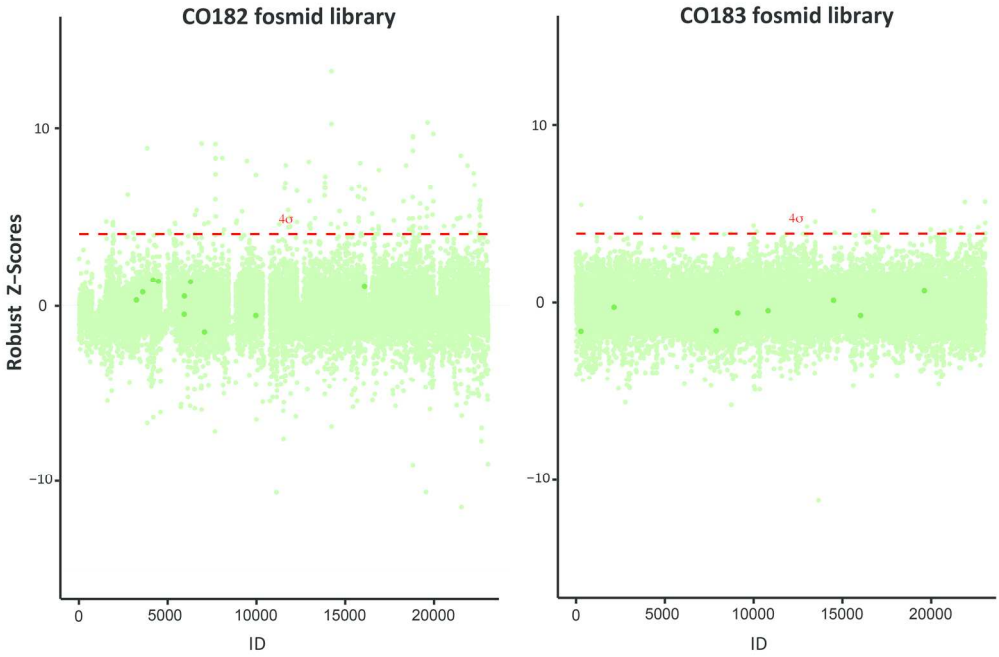

Metagenomic screening of coal-bed fosmid libraries, CO182 and CO183. CO182 and CO183 fosmid libraries were replicated in 384 well microplates and grown with 0.5% (v/w) HWKL for 48 hours followed by co-culture with the pET15 PemrR-gfp biosensor for 24 hours. Fluorescence measurements were recorded and normalized for plate-to-plate effects by robust Z-scores calculations.

171x115mm (300 x 300 DPI)

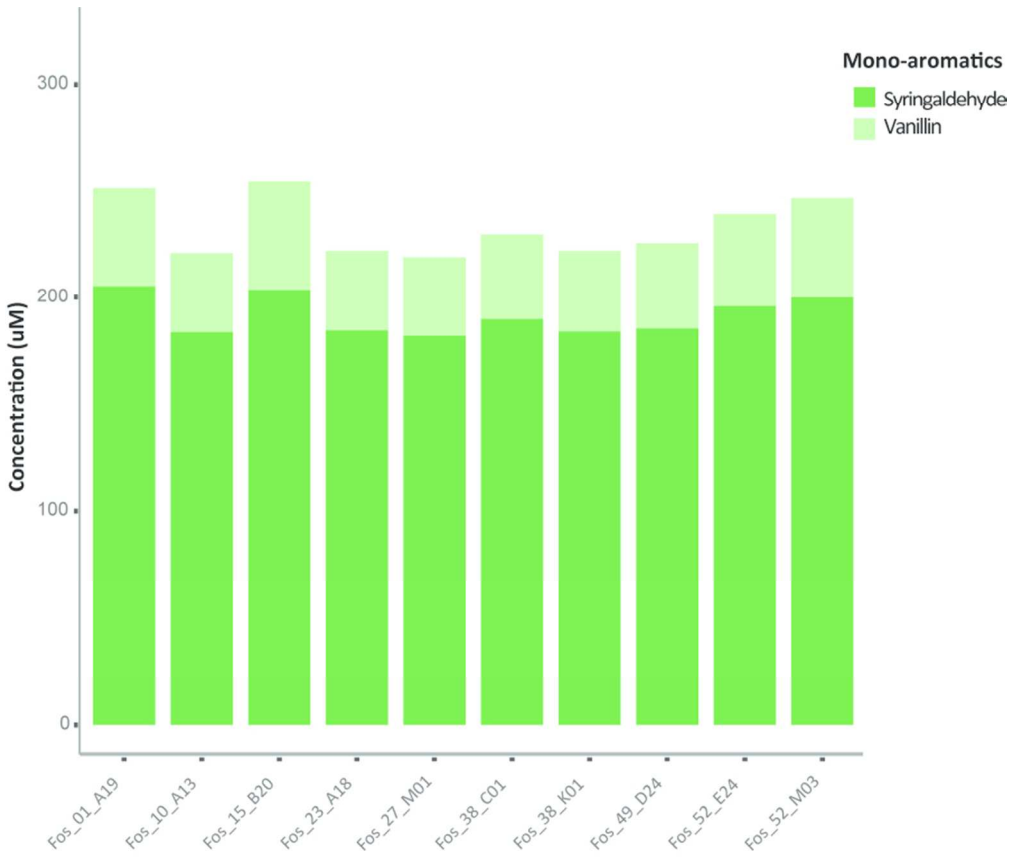

GC-MS confirmation of vanillin and syringaldehyde production on selected fosmid clones recovered in the re-screen with the improved pET15 biosensor. The top-5 fosmid clones (with the highest robust Z-score values) from each of the two coal bed libraries were chosen for GC-MS analysis. These fosmid clones were cultured on 0.5% (w/v) HWKL for 48 hours prior to extraction.

75x65mm (300 x 300 DPI)

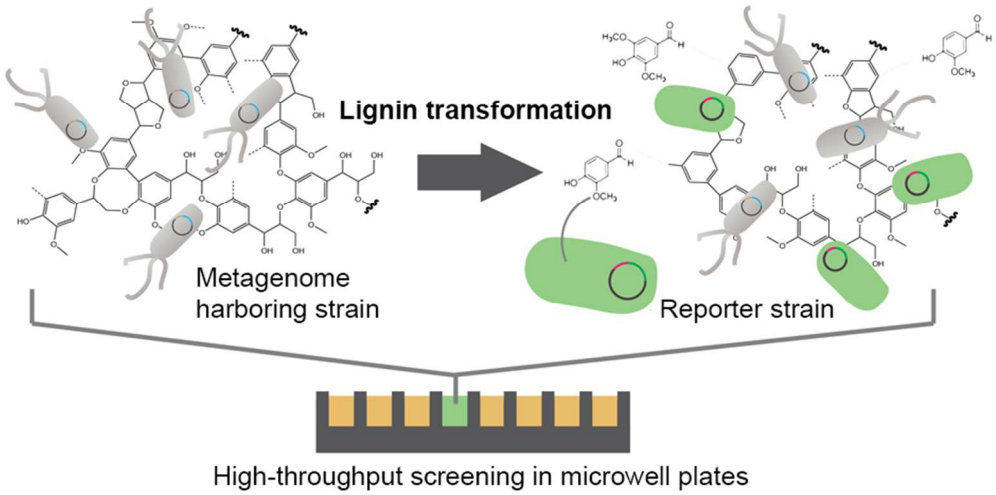

Table of contents graphic

80x39mm (300 x 300 DPI)